Interfacial Langmuir-Blodgett Layer of Functionalized Single-Walled Carbon Nanotubes for Efficient Glucose Sensing

Akash Gayakwad, V. Manjuladevi, and Raj Kumar Gupta

***Abstract*—The interfacial layer of single-walled carbon nanotubes (CNTs) introduced between the surface of the electrode and bio-ligands can enhance sensing performance by establishing amplified physical and chemical interaction between them. In this article, we report that an efficient glucose-sensing nanostratified layer can be created on the surface of the working electrode (gold surface) of an electrochemical platform by immobilizing glucose oxidase (GOx) on the highly organized Langmuir–Blodgett (LB) film of octadecylamine functionalized single-walled CNTs (ODACNTs). The amine group of ODACNTs provides stability to the Langmuir monolayer (LM) at the air-water (a/w) interface which is essential for the fabrication of highly ordered LB film. The sensing of glucose was performed in an aqueous medium using GOx immobilized layer onto the LB film and drop-casted film of ODACNTs modified working electrodes. The sensor fabricated using LB film modified electrodes offers a very wide concentration range (10 pM–1 mM), a very low limit of detection (LOD) (10 pM), and a sensitivity 2.8× better than that of drop-casted modified electrodes. The enhanced performance of LB film modified electrode is due to some coherent performance of organized nanotubes in the LB film as compared to a random network of the nanotubes in drop-casted film. The electrodes were characterized at different stages of sensing using grazing incidence X-ray diffraction, field emission scanning electron microscope (FESEM), Raman, and attenuated total internal reflection (ATR)-FTIR spectroscopies.**

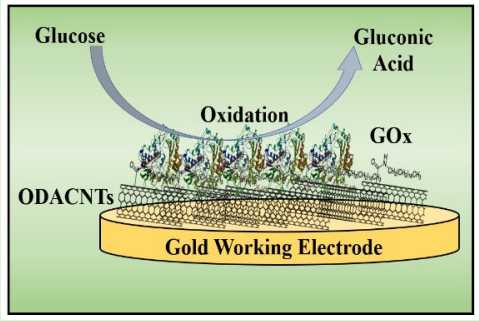

***Index Terms*—Electrochemical sensing, glucose, glucose oxidase (GOx), Langmuir–Blodgett (LB) film, octadecylamine functionalized single-walled carbon nanotubes (ODACNTs).**

I. Introduction

GLUCOSE is the major dietary source of energy from natural carbohydrates and is used as a processed food additive [1], [2]. From a clinical point of view, the level of blood glucose is a key indicator of diabetes and metabolic disorders. Hyperglycemia [3] and hypoglycemia in humans, both the conditions are clinically very severe. As per the International Diabetes Federation, almost ∼9.3% of the adult population is suffering from diabetes across the globe [4]. Apart from the biological perspective, glucose is also used in the chemical industry, cosmetic industry, bio-farming [5], and bio-fuel [6]. So, it becomes important to detect the glucose concentration in several such systems. An electrochemical biosensor can be one of the best sensing platforms to fulfill this requirement [7], [8]. Immobilization of the bio-active molecule on the surface of a working electrode for fabricating an electrochemical biosensor is the major issue. For developing an effective biosensor, immobilized bioactive molecules should have high reactivity and low interfacial resistance to react with the bioanalyte in the sensing environment [9], [10]. Various techniques have been used to immobilize the ligands on the electrode surface viz., cross-linker method [11], [12], self-assembly [13], deposition of layer-by-layer [14], [15], and Langmuir–Blodgett (LB) technique [16], [17], [18]. The LB technique provides a control on the orientational organization of the materials in the thin film and also on the thickness of the film [19].

Bioactive molecules can be made to adsorbed onto a molecular matrix of the LB template layer. Several studies were found in the literature on the biosensing application

Manuscript received 3 October 2023; accepted 23 October 2023. Date of publication 2 November 2023; date of current version 14 December 2023. This work was supported in part by the Science and Engineering Research Board (SERB) for Research Facilities under Grant CRG/2018/000755; and in part by the Department of Science and Technology (DST)-Fund for Improvement of Science and Technology (FIST) of the Department of Physics, BITS Pilani for X-Ray Diffractometer (XRD) Facility. The work of Akash Gayakwad was supported by the University Grants Commission (UGC)–Council of Scientific and Industrial Research (CSIR) under Grant 09/0719(12570)2021-EMR-I. The associate editor coordinating the review of this article and approving it for publication was Prof. Yu-Cheng Lin. *(Corresponding author: Raj Kumar Gupta.)*

The authors are with the Department of Physics, BITS Pilani, Pilani 333031, India (e-mail: p20190428@pilani.bits-pilani.ac.in; manjula@pilani.bits-pilani.ac.in.com; raj@pilani.bits-pilani.ac.in.com).

Digital Object Identifier 10.1109/JSEN.2023.3328059

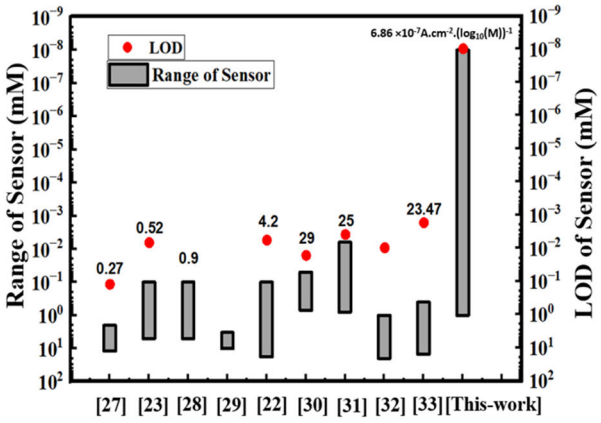

Fig. 1. Comparative plot of LOD, the concentration range of sensing and sensitivity. The number on top of each bar depicts the sensitivity of the glucose sensor in μA.cm^{-2}.mM^{-1}. The number along the x-axis represents the corresponding reference number.

of the LB films composed of polymer, carbon nanotubes (CNTs), graphene [20], organic molecules [21], Mxene [22], and nanocomposite of liquid crystal [23]. Conductivity, surface density, surface-to-volume ratio, and interaction with the bioactive molecule of the template layer are some of the factors that affect the performance of the electrochemical biosensor. Organic molecules such as liquid crystals and polymers have lower conductivity which reduces the overall performance of the electrical/electrochemical types of biosensors. The remarkable physicochemical properties of CNTs due to the large surface-to-volume ratio and high density of delocalized surface π-electrons make them a promising template layer for biosensing applications. The pristine CNTs are generally insoluble in organic solvent which makes the film processability difficult. Thus, the single-walled CNTs functionalized with organic ligands such as octadecylamine (ODACNTs) can disperse easily in organic solvent and are expected to form a stable Langmuir monolayer (LM) at the air-water (a/w) interface. Such stable monolayer can be transferred onto the active area of the device for sensing applications. The richness of delocalized surface π-electrons and –NH_2 groups of the ODACNTs can facilitate efficient binding with the biomolecules [24]. The reports in literature indicate that the LB films of several materials were employed for sensing glucose using some electrochemical techniques such as amperometry, cyclic voltammetry, and chronoamperometry. The limit of detection (LOD) was found to be in the range of micromolar. The detectable range of glucose concentration is reported to be narrow (Fig. 1).

In this article, we report an efficient glucose sensing based on the enzymatic interaction between the glucose oxidase (GOx) and glucose in an aqueous medium measured using an electrochemical technique. Strategically, we immobilized the GOx on the organized LB films of ODACNTs. The underlying ODACNTs facilitate not only an efficient binding of GOx but also a charge transfer mechanism during the electrochemical process between GOx and glucose. The sensing performance of the LB film-modified sensor is compared with that of the drop-casted ODACNTs-modified sensor. It was found that the LB-modified sensor has a wider concentration range of sensing (10 pM–1 mM) and 2.8× better sensitivity as compared to the drop-casted modified sensor. The efficient sensing of the LB modified layer can be attributed to the organized state of the CNTs leading to a coherent response to the electrochemical events [25], [26].

II. Experimental

ODACNTs were purchased from Carbon Solution Inc. (cat. # P5 SWNTs). ODACNTs are dispersible in an organic solvent such as chloroform; however, it is highly insoluble in an aqueous medium. GOx [aspergillus Niger (10KU)] was purchased from Sigma-Aldrich. D-glucose (purity > 99.5%) was purchased from Alfa Aesar. High-performance liquid chromatography (HPLC) grade (purity > 99%) chloroform was purchased from Merck. A Phosphate Buffer Saline (PBS) solution of pH ∼7 was prepared in the laboratory. A 0.03 mg·mL^{-1} chloroform solution of ODACNTs was ultrasonicated for 1 h to obtain a homogenous dispersion. Ultrapure Millipore water having a resistivity >18 MΩ-cm was used for all aqueous-related experiments.

Before fabrication of the template layer, the surface of the gold electrode was cleaned with cold piranha solution followed by successive rinsing using ultrapure water, ethanol, and chloroform. Then 150 μL of the chloroform solution of ODACNTs was drop-casted on the surface of the gold electrode (circular area 1.38 cm^2). About 30 min was allotted for the solvent chloroform to evaporate from the gold surface. An LB trough (KSV NIMA) of surface area 243 cm^2 was used to fabricate an LB film on the surface of the gold electrode. The detailed mechanism of the LB film fabrication is reported in our previous work [34], [35]. The chloroform solution of ODACNTs (1400 μL) was dispensed at the a/w interface between the barriers of the LB trough while the gold electrode was kept immersed in the water subphase. The solvent chloroform was allowed to evaporate from the water surface by waiting for about 10 min. Before deposition, three isocycles were executed to get a highly stable Langmuir film of ODACNTs. A single layer of LB film of ODACNTs was deposited on the surface of the gold electrode at a target surface pressure of 8 mN/m. The dipper speed was maintained at 5 mm/min. The transfer ratio was found to be ∼1.0. The gold electrodes deposited with drop-casted and LB films of ODACNTs were immersed in a 1 mg·mL^{-1} aqueous solution of the GOx for ∼8 h. The amine functionalization of ODACNTs facilitates immobilization of the GOx on the gold electrode. The GOx modified electrodes were taken out from the solution and rinsed gently with PBS solution to remove weakly bound GOx. Such functionalized electrodes were mounted in the electrochemical sensing setup and employed for glucose sensing in an aqueous PBS solution. The cyclic voltammetry technique was performed using CHI 1200 potentiostat with a three-electrode system—gold as working electrode, Ag/AgCl as reference electrode, and platinum wire as counter electrode. The cyclic voltammetry measurements were performed at the scan rate of 100 mV/s in a potential window of 0.6 to -0.6 V. For characterization of the functionalized layer, similar deposition mechanism was followed to deposit the films on silicon (Si)

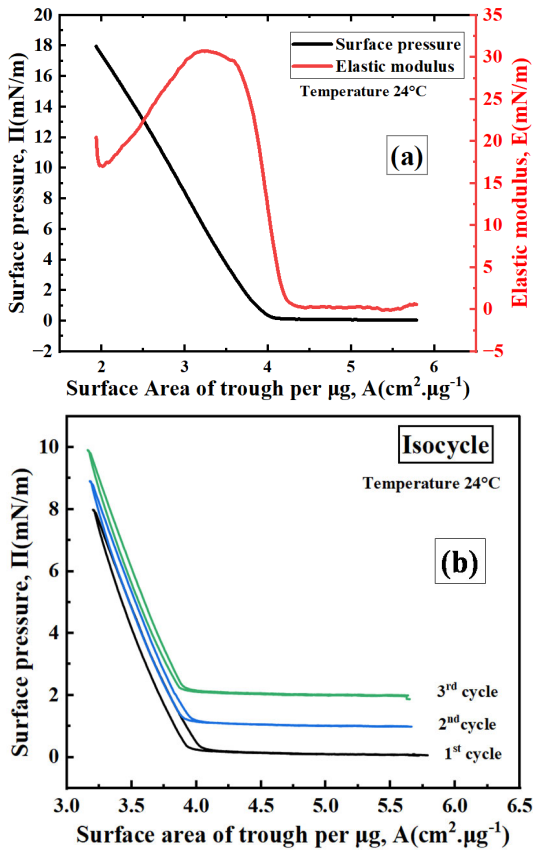

Fig. 2. (a) Π – A isotherm and E–A curve of Langmuir monolayer of ODACNTs at a/wW interface. (b) Isocycles of the monolayer at a/w interface. Each isocycle is shifted vertically with respect to each other by 1 mN/m for visual clarity.

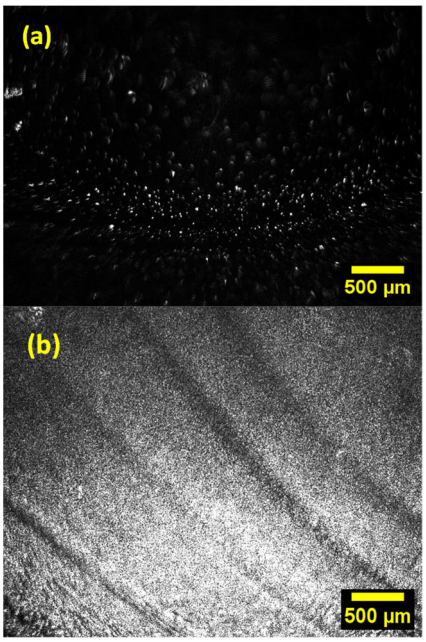

Fig. 3. BAM image of Langmuir monolayer of ODACNTs showing. (a) Gas and liquid-like phase coexistence. (b) Liquid-like phase. The temperature of the subphase was 24 °C.

wafers. Such functionalized Si wafers were characterized using grazing angle incident X-ray diffraction (GIXRD) technique (SmartLab, Rigaku). The Cu-K α radiation of wavelength 1.54 Å was incident at an angle of 0.3°. Raman spectra were collected using Horiba LabRam HR instrument operated at an excitation source of 633 nm. Morphological characterization was carried out using a field emission scanning electron microscope (FESEM) of FEI, Apreao LoVac instrument. Fourier transform infrared spectroscopy in attenuated total internal reflection (ATR) mode was performed using FTIR spectrometer (Shimadzu IRPrestige 21) equipped with ZnSe ATR crystal.

III. Results and Discussion

Surface pressure (Π)—surface area of trough per μg (A) isotherm of LM of ODACNT at a/w interface is shown in Fig. 2(a). The surface pressure remains negligible till the film is compressed at 4 cm^2. μg^{-1}. This can be considered as the gas phase of the LM of ODACNTs. The surface pressure rises sharply on compressing the film below 4 cm^2. μg^{-1}. This is the onset of liquid-like phase of the LM of ODACNTs. The surface pressure rises monotonically till the film is compressed completely in the trough. The isothermal in-plane elastic modulus (E) shows that the maximum value of E ($\sim$ 30 mN/m) in the liquid-like phase at around 3.1 cm^2. μg^{-1}. The reversal in trend of the E curve is due to change in slope in the Π-A isotherm. Here, the change in slope can be considered as the collapse of the monolayer. Therefore, the surface pressure of 8 mN/m at 3.2 cm^2. μg^{-1} corresponding to the highest E-value of liquid-like phase was as chosen for LB film deposition. The stability of the LM of ODACNTs at the a/w interface was studied by recording the isocycles [Fig. 2(b)] by repeated compression and expansion of the monolayer. As observed from the curve, there is a negligible hysteresis, and the expansion curves almost follow the compression curves. This indicates that the monolayer is stable against any dissolution in and irreversible aggregation on the water surface. The Brewster angle microscope (BAM) images of the LM of ODACNTs at the a/w interface is shown in Fig. 3. The gas and liquid-like phase coexistence region can be seen clearly as dark background and bright domains in Fig. 3(a), respectively. The bright texture as observed in Fig. 3(b) appears fluidic in nature which corresponds to the liquid-like phase of the LM of ODACNTs. The phase of the LM of ODACNTs in the A range of 4–3 cm^2. μg^{-1} can be considered liquid-like based on the maximum value of E (30 mN/m) [36], [37] and fluidic texture in the BAM images.

The LB and the drop-casted films on the gold electrodes were further modified by immobilizing GOx and used for sensing glucose in the aqueous PBS medium using cyclic voltammetry (Fig. 4). Results of cyclic voltammetry are shown in Fig. 5(a) and (b) for the drop-casted and LB film modified electrodes, respectively. The concentration range of glucose in the aqueous medium was chosen to be from 1 mM to 10 pM. It can be noted from Fig. 6 that the anodic current changes systematically with the change in the concentration of the glucose in the aqueous medium. The current response at anodic peak with different concentrations of glucose in the aqueous PBS solution (pH$\sim$7) corresponds to the oxidation of

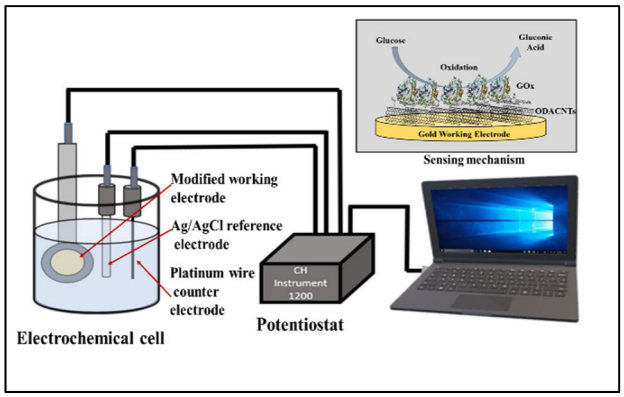

Fig. 4. Schematic illustration of sensing setup. The sensing mechanism is depicted in the inset.

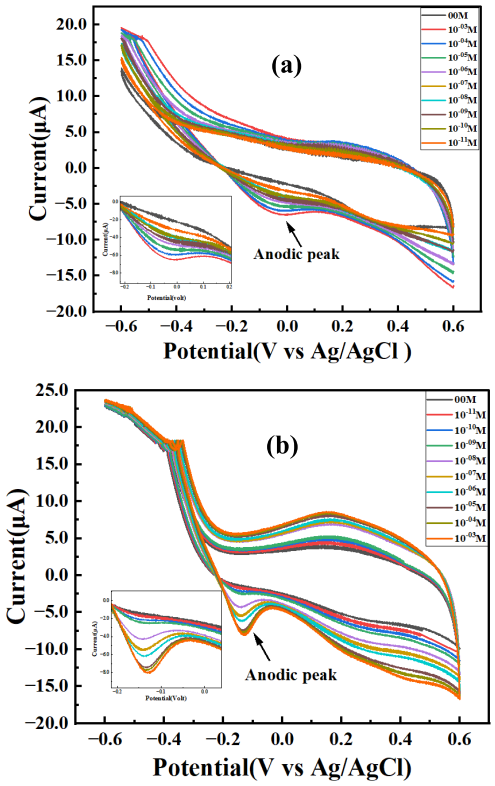

Fig. 5. Cyclic voltammetry on (a) drop-casted film, and (b) LB film of ODACNTs on gold-electrode immobilized with GOx and used for glucose sensing in aqueous PBS solution (∼pH 7.0).

the glucose as per given redox chemical reaction [38]

$$\text{Glucose} + O_2 \xrightarrow{\text{GOx}} \text{Gluconate} + H_2O_2$$
$$\text{Gluconate} + H_2O \rightarrow \text{Gluconic acid}.$$

The GOx facilitates the oxidation of glucose into gluconic acid and H_2O_2. The H_2O_2 is an electrochemically active species that gets oxidized at the working electrode leading to a change in current due to the transfer of electrons. The number of such oxidations depends on the concentration of glucose in the sensing medium. With the increase in the concentration of glucose in the aqueous medium, the magnitude of the anodic current increases systematically (Fig. 6). The glucose concentration below 10 pM does not

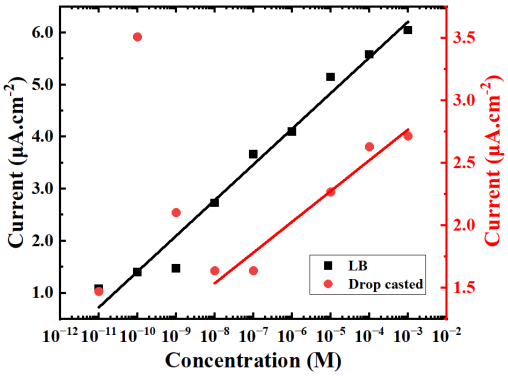

Fig. 6. Calibration curves for LB and drop-casted modified gold electrodes obtained by plotting anodic current as a function of concentration of glucose in aqueous PBS solution.

show any signatory change in the anodic current response. Therefore, 10 pM was considered as the limit-of-detection (LOD) for the LB-film-modified electrode. A calibration curve (Fig. 6) is drawn by plotting the anodic current as a function of the concentration of glucose in the aqueous medium for both the LB film and drop-casted film. It can be noted that the response curve obtained from the LB-film-modified electrode follows a linear trend for the entire concentration range, whereas the drop-casted modified electrode shows roughly linear variation only for the higher concentration range (10 nM–1 mM). For the lower concentration range (<10 nM), the drop-casted modified electrode shows random behavior. The sensitivity of the LB and drop-casted film modified sensor evaluated from the linear region of the calibration curve is found to be 6.86×10^{-7} and 2.46×10^{-7} A.cm^{-2}/log(M), respectively. The sensitivity due to the LB film was found to be 2.8× better than that of drop-casted film. It is observed from the literature that the sensing performance of LB film of CNTs is much better due to the alignment of CNTs in the LB film. The coherent performance of the aligned nanotubes can enhance the charge transfer mechanism and density of surface active hot-spots. However, such enhancement was not observed in the drop-casted film due to the random network of the nanotubes and higher thickness of the film [39], [40].

The functional layers were characterized using FESEM, XRD, and Raman spectroscopy before and after interaction with the glucose. The morphology of the film before and after interaction with the glucose is shown in Fig. 7. The bundles of ODACNTs are clearly seen in the image with sharp edges [Fig. 7(a)]. With the deposition of GOx, the overall sharpness of the bundles reduces and a layer appears to be seen on the surface of the nanotube film [Fig. 7(b)]. After interaction with glucose, a thick layer is found over the surface of underlying nanotubes [Fig. 7(c)]. The FESEM image of the drop-casted film showed a random network of the nanotubes.

The GIXRD curves of the film at different stages are shown in Fig. 8. The characteristic peaks for Si are observed at 42.5° and 47.3°. The 2θ peaks corresponding to the ODACNTs are found at 21.5° and 23.7° [41]. With the immobilization of the GOx, no significant change in the peak position was observed. However, after interaction with the glucose in an aqueous PBS

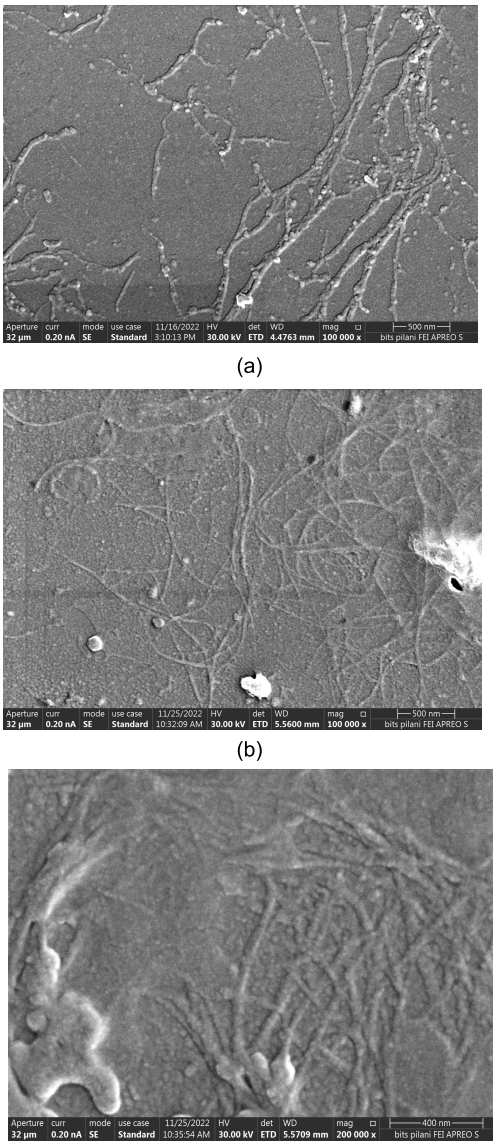

Fig. 7. (a) FESEM images of LB film of ODACNTs on silicon substrate. (b) FESEM image of GOx on LB film of ODACNTs on silicon substrate. (c) FESEM image of Glucose adsorbed GOx on LB film of ODACNTs on silicon substrate.

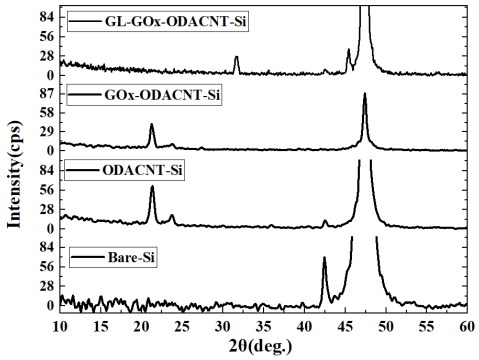

Fig. 8. GIXRD on Silicon substrate at different stages at 0.3° incident angle.

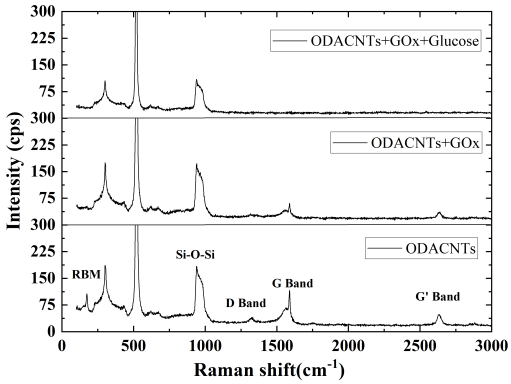

Fig. 9. RAMAN spectra performed on Silicon substrate at different stages at 633 nm excitation.

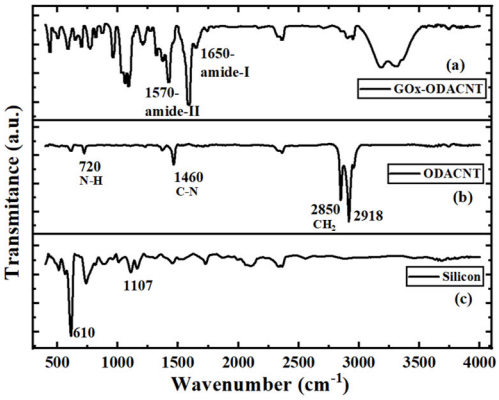

Fig. 10. FTIR-ATR spectra of GOx-ODACNT.

medium, the signature peaks disappear, and the new peaks at 31.7° and 45.4° were observed. These new peaks are due to the salts of the PBS buffer solution.

The Raman spectra of the film at different stages are shown in Fig. 9. The characteristic peaks for the ODACNTs such as G-bands (G^+ and G^- at 1588 and 1560 cm^{-1}, respectively), D-band (1353 cm^{-1}), G'-band (2640 cm^{-1}), and RBM (175 cm^{-1}) were seen in the spectrum [42], [43]. The splitting of the G-band into G^+ (longitudinal wave mode) and G^- (transverse wave mode) can be clearly seen from the spectrum. The characteristics peaks of Si were observed at 301, 520, and 976 cm^{-1} [44]. Due to the immobilization of GOx on the ODACNTs, the RBM vanishes completely which may indicate that the binding of GOx with the CNTs is strong enough to eliminate the radial breathing mode. The strength of D and G bands reduces with the GOx functionalization; however, all ODACNTs specific bands disappear after the interaction of GOx with glucose in the aqueous medium.

The defect density in the ODACNTs can be estimated from the ratio of the intensity of the D to G band (i.e., I_D/I_G). The defect density of the pure ODACNTs layer and GOx immobilized layer was calculated to be 0.64 and 0.70, respectively. The marginal change in the defect density indicates that the presence of defects in the nanotubes does not a play major role in facilitating the adsorption of the GOx. The GOx binds to the nanotubes primarily due to the $\pi - \pi$ interaction. The results of GIXRD and Raman spectra complement each other.

Since the presence of GOx was not clearly observed by Raman spectroscopy, the FTIR spectroscopy in ATR mode was performed on GOx immobilized LB film of ODACNTs

(Fig. 10). The presence of amide peaks at 1570 cm^{-1} (amide-I) and 1650 cm^{-1} (amide-II) [45] was observed from the spectrum of GOx immobilized on LB film of ODACNTs [Fig. 10(a)]. The LB film of ODACNTs shows primarily N–H (wagging) at 720 cm^{-1}, C–N (stretching) at 1460 cm^{-1}, CH_2 (sym. stretching) at 2850 cm^{-1}, and CH_2 (asym. stretching) at 2918 cm^{-1} [46].

IV. Conclusion

This report claims a very low value of LOD, wider concentration range, and higher sensitivity toward glucose through the enzymatic interaction between GOx and glucose as measured using cyclic voltammetry technique. It is found that the presence of the interfacial LB film of ODACNTs between the gold surface and the GOx plays a crucial role in enhancing the sensing merits of glucose in the aqueous medium. The sensor modified with LB film offers a very wide concentration range for the detection of glucose (10 pM–1 mM) and a LOD of 10 pM. The sensitivity due to LB film is about 2.8× better than that of drop-casted film. The LB film offers an organized assembly of the nanotubes. Such organized assembly may perform coherently to yield better sensing performance as compared to the random orientation of the network of the nanotubes in drop-casted film.

References

[1] K. H. Nam, "Glucose isomerase: Functions, structures, and applications," *Appl. Sci.*, vol. 12, no. 1, p. 428, Jan. 2022, doi: 10.3390/app12010428.

[2] E. B. Jackson, "Use of glucose syrups in the food industry," in *Handbook of Starch Hydrolysis Products and their Derivatives*. New York, NY, USA: Springer, 1995, pp. 245–268, doi: 10.1007/978-1-4615-2159-4_9.

[3] M. Mouri and M. Badireddy, "Hyperglycemia," in *Mader's Reptile and Amphibian Medicine and Surgery*. Treasure Island, FL, USA: Statpearls Publishing, Apr. 2022, pp. 1314–1315, doi: 10.1016/B978-0-323-48253-0.00155-0.

[4] P. Saeedi et al., "Global and regional diabetes prevalence estimates for 2019 and projections for 2030 and 2045: Results from the international diabetes federation diabetes atlas, 9th edition," *Diabetes Res. Clin. Pract.*, vol. 157, Nov. 2019, Art. no. 107843, doi: 10.1016/j.diabres.2019.107843.

[5] P. M. Rutherford and N. G. Juma, "Effect of glucose amendment on microbial biomass, spelling fertilizer ^{15}N-recovery and distribution in a barley-soil-system," *Biol Fertil Soils*, vol. 12, no. 4, pp. 228–232, Jan. 1992, doi: 10.1007/BF00336037.

[6] H. Sakai et al., "A high-power glucose/oxygen biofuel cell operating under quiescent conditions," *Energy Environ. Sci.*, vol. 2, no. 1, pp. 133–138, 2009, doi: 10.1039/b809841g.

[7] E. Witkowska Nery, M. Kundys, P. S. Jelen, and M. Jönsson-Niedziólka, "Electrochemical glucose sensing: Is there still room for improvement?" *Anal. Chem.*, vol. 88, no. 23, pp. 11271–11282, Dec. 2016, doi: 10.1021/acs.analchem.6b03151.

[8] H. Teymourian, A. Barfidokht, and J. Wang, "Electrochemical glucose sensors in diabetes management: An updated review (2010–2020)," *Chem. Soc. Rev.*, vol. 49, no. 21, pp. 7671–7709, 2020, doi: 10.1039/d0cs00304b.

[9] Q. Liu et al., "Highly sensitive and wearable In_2O_3 nanoribbon transistor biosensors with integrated on-chip gate for glucose monitoring in body fluids," *ACS Nano*, vol. 12, no. 2, pp. 1170–1178, Feb. 2018, doi: 10.1021/acsnano.7b06823.

[10] N. Gao et al., "Graphene electrochemical transistor incorporated with gel electrolyte for wearable and non-invasive glucose monitoring," *Analytica Chim. Acta*, vol. 1239, Jan. 2023, Art. no. 340719, doi: 10.1016/j.aca.2022.340719.

[11] A. Fang, H. T. Ng, and S. F. Y. Li, "A high-performance glucose biosensor based on monomolecular layer of glucose oxidase covalently immobilised on indium-tin oxide surface," *Biosens Bioelectron*, vol. 19, no. 1, pp. 43–49, Oct. 2003, doi: 10.1016/S0956-5663(03)00133-7.

[12] Y. Liu, D. Yu, C. Zeng, Z. Miao, and L. Dai, "Biocompatible graphene oxide-based glucose biosensors," *Langmuir*, vol. 26, no. 9, pp. 6158–6160, May 2010, doi: 10.1021/la100886x.

[13] H. Wu, Y. Saito, G. Yoshizaki, Y. Yoshiura, H. Ohnuki, and H. Endo, "Study on the development of carbon nanotube enhanced biosensor for gender determination of fish," *Sens. BioSensing Res.*, vol. 35, Feb. 2022, Art. no. 100474, doi: 10.1016/j.sbsr.2022.100474.

[14] S. Komathi, A. I. Gopalan, and K.-P. Lee, "Fabrication of a novel layer-by-layer film based glucose biosensor with compact arrangement of multi-components and glucose oxidase," *Biosensors Bioelectron.*, vol. 24, no. 10, pp. 3131–3134, Jun. 2009, doi: 10.1016/j.bios.2009.03.013.

[15] T. F. Schmidt, L. Caseli, T. Viitala, and O. N. Oliveira, "Enhanced activity of horseradish peroxidase in Langmuir–Blodgett films of phospholipids," *Biochimica et Biophysica Acta (BBA)-Biomembranes*, vol. 1778, no. 10, pp. 2291–2297, Oct. 2008, doi: 10.1016/j.bbamem.2008.05.012.

[16] S. K. Sharma, R. Singhal, B. D. Malhotra, N. Sehgal, and A. Kumar, "Langmuir–Blodgett film based biosensor for estimation of galactose in milk," *Electrochimica Acta*, vol. 49, no. 15, pp. 2479–2485, Jun. 2004, doi: 10.1016/j.electacta.2004.01.024.

[17] R. Singhal, W. Takashima, K. Kaneto, S. B. Samanta, S. Annapoorni, and B. D. Malhotra, "Langmuir–Blodgett films of poly(3-dodecyl thiophene) for application to glucose biosensor," *Sens Actuators B, Chem*, vol. 86, no. 1, pp. 42–48, Aug. 2002, doi: 10.1016/S0925-4005(02)00145-4.

[18] H. Ohnuki, T. Saiki, A. Kusakari, H. Endo, M. Ichihara, and M. Izumi, "Incorporation of glucose oxidase into Langmuir–Blodgett films based on Prussian blue applied to amperometric glucose biosensor" *Langmuir*, vol. 23, no. 8, pp. 4675–4681, Apr. 2007, doi: 10.1021/la063175g.

[19] L. Caseli, "Enzymes immobilized in Langmuir–Blodgett films: Why determining the surface properties in Langmuir monolayer is important?" *Anais da Academia Brasileira de Ciencias*, vol. 90, pp. 631–644, Jan. 2018, doi: 10.1590/0001-3765201720170453.

[20] S. S. Alabsi, A. Y. Ahmed, J. O. Dennis, M. H. M. Khir, and A. S. Algamili, "A review of carbon nanotubes field effect-based biosensors," *IEEE Access*, vol. 8, pp. 69509–69521, 2020, doi: 10.1109/access.2020.2987204.

[21] H. Tsuzuki et al., "A novel glucose sensor with a glucose oxidase monolayer immobilized by the Langmuir–Blodgett technique," *Chem. Lett.*, vol. 17, no. 8, pp. 1265–1268, Aug. 1988, doi: 10.1246/cl.1988.1265.

[22] R. B. Rakhi, P. Nayak, C. Xia, and H. N. Alshareef, "Novel amperometric glucose biosensor based on MXene nanocomposite," *Sci. Rep.*, vol. 6, no. 1, p. 36422, Nov. 2016, doi: 10.1038/srep36422.

[23] K.-H. Wang, J.-Y. Wu, L.-H. Chen, and Y.-L. Lee, "Architecture effects of glucose oxidase/Au nanoparticle composite Langmuir–Blodgett films on glucose sensing performance," *Appl. Surf. Sci.*, vol. 366, pp. 202–209, Mar. 2016, doi: 10.1016/j.apsusc.2016.01.047.

[24] C. Ménard-Moyon, K. Kostarelos, M. Prato, and A. Bianco, "Functionalized carbon nanotubes for probing and modulating molecular functions," *Chem. Biol.*, vol. 17, no. 2, pp. 107–115, Feb. 2010, doi: 10.1016/j.chembiol.2010.01.009.

[25] P. Taneja, V. Manjuladevi, K. K. Gupta, and R. K. Gupta, "Detection of cadmium ion in aqueous medium by simultaneous measurement of piezoelectric and electrochemical responses," *Sens. Actuators B, Chem.*, vol. 268, pp. 144–149, Sep. 2018, doi: 10.1016/j.snb.2018.04.091.

[26] S. U. Khan, J. R. Pothnis, and J.-K. Kim, "Effects of carbon nanotube alignment on electrical and mechanical properties of epoxy nanocomposites," *Compos. A, Appl. Sci. Manuf.*, vol. 49, pp. 26–34, Jun. 2013, doi: 10.1016/j.compositesa.2013.01.015.

[27] A. Márquez, C. Jiménez-Jorquera, C. Domínguez, and X. Muñoz-Berbel, "Electrodepositable alginate membranes for enzymatic sensors: An amperometric glucose biosensor for whole blood analysis," *Biosensors Bioelectron.*, vol. 97, pp. 136–142, Nov. 2017, doi: 10.1016/j.bios.2017.05.051.

[28] K.-H. Wang, M.-J. Syu, C.-H. Chang, and Y.-L. Lee, "Immobilization of glucose oxidase by Langmuir–Blodgett technique for fabrication of glucose biosensors: Headgroup effects of template monolayers," *Sens. Actuators B, Chem.*, vol. 164, no. 1, pp. 29–36, Mar. 2012, doi: 10.1016/j.snb.2012.01.056.

[29] A. J. Bandodkar et al., "Re-usable electrochemical glucose sensors integrated into a smartphone platform," *Biosensors Bioelectron.*, vol. 101, pp. 181–187, Mar. 2018, doi: 10.1016/j.bios.2017.10.019.

[30] V. Myndrul et al., "MXene nanoflakes decorating ZnO tetrapods for enhanced performance of skin-attachable stretchable enzymatic electrochemical glucose sensor," *Biosensors Bioelectron.*, vol. 207, Jul. 2022, Art. no. 114141, doi: 10.1016/j.bios.2022.114141.

[31] P.-H. Lin, S.-C. Sheu, C.-W. Chen, S.-C. Huang, and B.-R. Li, "Wearable hydrogel patch with noninvasive, electrochemical glucose sensor for natural sweat detection," *Talanta*, vol. 241, May 2022, Art. no. 123187, doi: 10.1016/j.talanta.2021.123187.

[32] Q. Wang et al., "Dual confinement of high-loading enzymes within metal-organic frameworks for glucose sensor with enhanced cascade biocatalysis," *Biosensors Bioelectron.*, vol. 196, Jan. 2022, Art. no. 113695, doi: 10.1016/j.bios.2021.113695.

[33] W. Lipińska, K. Siuzdak, J. Karczewski, A. Dolega, and K. Grochowska, "Electrochemical glucose sensor based on the glucose oxidase entrapped in chitosan immobilized onto laser-processed Au-Ti electrode," *Sens. Actuators B, Chem.*, vol. 330, Mar. 2021, Art. no. 129409, doi: 10.1016/j.snb.2020.129409.

[34] R. K. G. Manjuladevi, "Ultrathin films," in *Comprehensive Guide for Nanocoatings Technology*, M. Aliofkhazraei, Ed. New York, NY, USA: NOVA, 2014.

[35] M. Poonia, V. Manjuladevi, and R. K. Gupta, "Ultrathin films of functionalised single-walled carbon nanotubes: A potential bio-sensing platform," *Liquid Crystals*, vol. 47, no. 8, pp. 1204–1213, Jun. 2020, doi: 10.1080/02678292.2020.1718788.

[36] A. Ladniak, M. Jurak, and A. E. Wiacek, "Langmuir monolayer study of phospholipid DPPC on the titanium dioxide-chitosan-hyaluronic acid subphases," *Adsorption*, vol. 25, no. 3, pp. 469–476, Apr. 2019, doi: 10.1007/s10450-019-00037-1.

[37] K. Choudhary, J. Kumar, P. Taneja, R. K. Gupta, and V. Manjuladevi, "Langmuir–Blodgett films of stearic acid deposited on substrates at different orientations relative to compression direction: Alignment layer for nematic liquid crystal," *Liquid Crystals*, vol. 44, no. 10, pp. 1592–1599, Aug. 2017, doi: 10.1080/02678292.2017.1306890.

[38] L. C. Clark and C. Lyons, "Electrode systems for continuous monitoring in cardiovascular surgery," *Ann. New York Acad. Sci. USA*, vol. 102, no. 1, pp. 29–45, Oct. 1962, doi: 10.1111/j.1749-6632.1962.tb13623.x.

[39] M. Poonia et al., "Ultrathin films of single-walled carbon nanotubes: A potential methane gas sensor," *Sci. Adv. Mater.*, vol. 7, no. 3, pp. 455–462, Mar. 2015, doi: 10.1166/sam.2015.1989.

[40] K. Choudhary, V. Manjuladevi, R. K. Gupta, P. Bhattacharyya, A. Hazra, and S. Kumar, "Ultrathin films of TiO_2 nanoparticles at interfaces," *Langmuir*, vol. 31, no. 4, pp. 1385–1392, Feb. 2015, doi: 10.1021/la503514p.

[41] M. C. G. Pedrosa, J. C. Dutra Filho, L. R. D. Menezes, and E. O. D. Silva, "Chemical surface modification and characterization of carbon nanostructures without shape damage," *Mater. Res.*, vol. 23, no. 2, 2020, Art. no. e20190493, doi: 10.1590/1980-5373-mr-2019-0493.

[42] S. Costa, E. Borowiak-Palen, M. Kruszynska, A. Bachmatiuk, and R. J. Kalenczuk, "Characterization of carbon nanotubes by Raman spectroscopy," *Mater. Sci.-Poland*, vol. 26, no. 2, pp. 433–441, 2008.

[43] L. Ma, G. Wang, and J. Dai, "Preparation of a functional reduced graphene oxide and carbon nanotube hybrid and its reinforcement effects on the properties of polyimide composites," *J. Appl. Polym. Sci.*, vol. 134, no. 11, pp. 1–9, Mar. 2017, Art. no. 44575, doi: 10.1002/app.44575.

[44] V. Mankad, S. K. Gupta, P. K. Jha, N. N. Ovsyuk, and G. A. Kachurin, "Low-frequency Raman scattering from Si/Ge nanocrystals in different matrixes caused by acoustic phonon quantization," *J. Appl. Phys.*, vol. 112, no. 5, pp. 1–8, Sep. 2012, Art. no. 054318, doi: 10.1063/1.4747933.

[45] C. Chey, Z. Ibupoto, K. Khun, O. Nur, and M. Willander, "Indirect determination of mercury ion by inhibition of a glucose biosensor based on ZnO nanorods," *Sensors*, vol. 12, no. 11, pp. 15063–15077, Nov. 2012, doi: 10.3390/s121115063.

[46] B. R. C. de Menezes et al., "Effects of octadecylamine functionalization of carbon nanotubes on dispersion, polarity, and mechanical properties of CNT/HDPE nanocomposites," *J. Mater. Sci.*, vol. 53, no. 20, pp. 14311–14327, Oct. 2018, doi: 10.1007/s10853-018-2627-3.

Akash Gayakwad received the B.Sc. and M.Sc. degrees in physics from Devi Ahilya Vishwavidyalaya, Indore, India, in 2015 and 2017, respectively.

He joined BITS Pilani as a Ph.D. Scholar under the Supervision of Prof. R. K. Gupta, in 2020. His research interests include Langmuir monolayer and Langmuir–Blodgett films of liquid crystal, nanomaterials, and their sensing application.

Mr. Gayakwad was awarded with CSIR-NET Fellowship in December 2019.

V. Manjuladevi received the Ph.D. degree in physical sciences from Raman Research Institute, Bangalore, India, in 2004.

She has worked as a Postdoctoral Fellow with Trinity College Dublin, Dublin, Ireland, from 2004 to 2006. In 2006, she joined as a Faculty Member with the Department of Physics, BITS Pilani, Pilani, India. Currently, she is working as a Professor with the Department of Physics. She has guided four Ph.D. students and published more than 60 research article in peer reviewed journals. She works in the field of liquid crystal and their application for display and non-display devices such as smart windows. Her research interests include surface plasmon resonance-based devices, thin films of organic and nanomaterials, sensing.

Raj Kumar Gupta received the Ph.D. degree in physical sciences from Raman Research Institute, Bangalore, India, in 2005.

He joined with the Department of Physics, BITS Pilani, Pilani, India in 2005 and where he currently working as a Professor with the Department of Physics. He has guided six Ph.D. students and published more than 70 research article in peer reviewed. His research interests include the surface plasmon resonance-based devices, thin films of organic and nanomaterials and sensing.